ELSEVIER

Journal of Food Engineering 47 (2001) 69–79

JOURNAL OF FOOD ENGINEERING

www.elsevier.com/locate/jfoodeng

Weight loss during freezing and storage of unpackaged foods

L.A. Campañone [a,b], V.O. Salvadori [a,b,*], R.H. Mascheroni [a,b]

[a] CIDCA (Centro de Investigación y Desarrollo en Criotecnología de Alimentos, UNLP–CONICET) 47 y 116 – (1900) La Plata, Argentina
[b] MODIAL, Facultad de Ingeniería, Universidad Nacional de La Plata, La Plata, Argentina

Received 13 September 1999; accepted 8 June 2000

Abstract

Dehydration of unwrapped foods occurs during freezing and frozen storage. Coupled heat and mass balances were proposed incorporating solidification of water and sublimation of ice. The mathematical model was solved using an implicit finite-differences method, with a variable grid to follow the moving sublimation front. The model evaluates temperature and water concentration profiles and was used to predict the kinetics of weight loss for different products. Model predictions were favourably compared against experimental data on weight loss during storage of unwrapped meat, potato and tylose. © 2000 Elsevier Science Ltd. All rights reserved.

Keywords: Frozen foods; Weight loss; Numerical models; Freezing; Storage

1. Introduction

When unwrapped foods are frozen and/or stored in the frozen state or with a non-adhering packaging, weight losses take place due to sublimation of the surface ice.

Ice sublimation produces a dehydrated surface layer that changes the appearance, colour, texture and taste. Furthermore, in the industry, this weight loss becomes an important quality and economic factor.

These losses have two different origins, but their effects are cumulative:

- During freezing, the food surface has a higher temperature than the circulating air, and, thus, the surface water vapour pressure, P_{va}, is also higher than that of air. The lower the freezing speed, the slower the decrease in surface temperature, and this results in greater differences of vapour pressure between food and air. In addition, the duration of the freezing process will be longer, both factors increasing the weight loss. The higher the cooling speed, the lesser the sublimation.
- During storage, room temperature fluctuations are transferred, delayed in time, to the stored goods. Thus, there will be alternating periods in which their surface temperature is higher than the room temperature, with subsequent ice sublimation. The cumulative weight lost throughout long storage periods may cause an important quality loss. This second effect is usually much more important than the one caused during freezing.

Ice sublimation has been surveyed by several authors in different systems: in freeze-drying (Mellor, 1974; Kochs, Körber, Nunner, & Heschel, 1990), in geomorphology (Aguirre Puente, Frémond, & Comini, 1978) and in the case of frozen products several experimental studies have been published: weight losses of lamb (Pham & Willix, 1984), tylose and beef (Sukhwal & Aguirre Puente, 1983), potatoes (Lambrinos & Aguirre Puente, 1983) and beef and pork (Méndez Bustabad, 1999).

Theoretical models were proposed to predict simultaneous heat and mass transfer during freezing and storage but, in most of the published works, semi-empiric models were used. Aguirre Puente and Sukhwal (1983) presented a detailed description of the heat and mass balances that characterize the system, but without solving them numerically; meanwhile Pham and Willix (1984) suggested the use of simple equations based on drying theory and on the use of the psychometric chart to calculate weight loss only during frozen storage. They considered a dried layer of constant thickness and its resistance to heat and mass transfer; a similar approximation is made by Tocci and Mascheroni (1995a) in

* Corresponding author. Tel.: +54-221-4249287; fax: +54-221-4249287.
E-mail address: vosalvad@volta.ing.unlp.edu.ar (V.O. Salvadori).

PII: S0260-8774(00)00101-1

Nomenclature

A	area, m^2
b	index indicating surface position
C	molar concentration, mol/m^3
Cp	specific heat, J/(kg °C)
D_{ef}	effective diffusion coefficient of water vapour, m^2/s
D_w	diffusion coefficient of water, m^2/s
f_{ads}	adsorbed ice fraction, (kg of ice)/(kg of dried solid)
GI	geometric index, its value is 0 for slabs, 1 for cylinders and 2 for spheres
h	heat transfer coefficient, $W/(m^2\ °C)$
HR	relative humidity, %
i	position index
k	thermal conductivity, W/(m °C)
k_m	mass transfer coefficient (referred to vapour water driving force), m/s
k'_m	mass transfer coefficient (referred to liquid water driving force), m/s
L	half-thickness or radius, m
L_s	sublimation heat of ice, J/kg
m	index indicating sublimation front position
m_s	sublimated mass by unit volume, kg/m^3
n	time index
P	pressure, Pa
P_{sat}	vapour saturation pressure, Pa
Pr	Prandtl number
R	universal gas constant, 8.31 J/(mol K)
Re	Reynolds number
t	time, s (or min)
T	temperature, °C
U	temperature or concentration in Eqs. (14)–(16)
v	air velocity, m/s
V	thermal conductivity or diffusion coefficient in Eq. (17)
Vol	volume, m^3
w	ice content, (kg of ice)/(kg of food)
WL1	weight loss during step 1, (kg of water)/(kg of food)
WL2	weight loss during step 2, (kg of water)/(kg of food)
x	spatial coordinate, m
x_1	moving sublimation front position, m
Y_0	initial water content, (kg of water)/(kg of food)
Δx	constant spatial increment, frozen zone, m
Δx_2	variable spatial increment, within the frozen zone, m
Δx_4	variable spatial increment, within the dehydrated zone, m
Δt	time increment, s

Greek symbols

ρ	density, kg/m^3
ε	porosity
τ	tortuosity

Subscripts

a	air
d	dehydrated
ef	effective
eq	equilibrium
i	initial
if	initial freezing
L	surface
sat	saturation
va	water vapour
w	water

their study of heat and mass transfer during food freezing.

The objectives of this work were:

- to develop a physical model and to implement the related numerical method that enables us to account for the influence of food characteristics and process variables on the freezing time, weight loss and on the growth rate of the dehydrated surface layer,
- to verify the predictions of the model against experimental data of freezing times of unwrapped foods and their weight loss during frozen storage.

In that sense, coupled heat and mass balances were solved. The thermophysical properties were considered as being variable with temperature and the physical state of the product (unfrozen, frozen or dehydrated). Two phase changes were included in the model: liquid to solid and solid to vapour. Solidification is considered through a variable apparent heat capacity and a numerical method that uses a fixed grid (Cleland, 1990). Meanwhile ice sublimation can be adequately modelled by a moving front and the same numerical method, but with variable grid, because of its very low displacement rate as compared to that of the solidification process (Marshall, Rey, & Smith, 1986).

The model has been implemented in FORTRAN and the predictions have been contrasted with the bibliographical information for meat, tylose and potato.

2. Theory

During the freezing and frozen storage of unwrapped foods, they lose weight due to the environmental interaction. When frozen water sublimates a porous dehydrated layer is formed on the food surface, which alters the food physical and organoleptic characteristics.

During the freezing, two-state phase changes take place simultaneously: the free liquid water is frozen and the superficial water sublimates. In the case of frozen storage, only one phase change takes place, the sublimation of superficial ice.

From a physical point of view, food can be considered as a combination of a solid matrix, an aqueous phase and a gaseous phase (air and water vapour). For the freezing process, the food can be divided in three zones: unfrozen, frozen and dehydrated. During the storage, there are only two zones: frozen and dehydrated; from the mathematical point of view, the storage stage can be considered as a special case of the most general formulation (freezing stage) and needs no special development.

A complete mathematical model has to solve the heat transfer (freezing) and the mass transfer (weight loss) simultaneously. As the industrial freezing process begins with the food at temperatures higher than T_{if} the model must consider also the weight loss during the initial refrigeration step.

In this work, the analysis was performed for regular unidimensional geometries (plane plate, infinite cylinder, sphere). A general formulation could be developed which accounts for each of these three geometries by means of the geometric index GI. The analysis is divided into two steps: 1 and 2.

Step 1. For temperatures higher than the initial freezing point T_{if}, the following balances are valid for all the food ($0 \leqslant x < L$), where x is the axial or radial coordinate:

$$\rho \mathrm{Cp} \frac{\partial T}{\partial t} = \frac{\partial k}{\partial x}\frac{\partial T}{\partial x} + k\frac{\partial^2 T}{\partial x^2} + \mathrm{GI}\frac{k}{x}\frac{\partial T}{\partial x}, \tag{1}$$

$$\frac{\partial C_w}{\partial t} = \frac{\partial D_w}{\partial x}\frac{\partial C_w}{\partial x} + D_w\frac{\partial^2 C_w}{\partial x^2} + \mathrm{GI}\frac{D_w}{x}\frac{\partial C_w}{\partial x} \tag{2}$$

with the following boundary conditions:

$$x = 0: \qquad \frac{\partial T}{\partial x} = 0, \tag{3}$$

$$x = L: \qquad -k\frac{\partial T}{\partial x} = h(T - T_a), \tag{4}$$

$$x = 0: \qquad \frac{\partial C_w}{\partial x} = 0, \tag{5}$$

$$x = L: \qquad -D_w\frac{\partial C_w}{\partial x} = k'_m(C_w - C_{eq}). \tag{6}$$

Step 2. When the surface temperature T_L reaches T_{if}, freezing and ice sublimation begin and different zones need to be considered

(2.1). For the unfrozen and frozen zones ($0 \leqslant x < x_1$), Eq. (1) was applied to calculate the temperature profile, being x_1 the position of the sublimation front.

(2.2) For the dehydrated zone ($x_1 < x \leqslant L$), Eq. (7) was applied to calculate temperatures

$$\rho_d \mathrm{Cp}_d \frac{\partial T}{\partial t} = \frac{\partial k_d}{\partial x}\frac{\partial T}{\partial x} + k_d\frac{\partial^2 T}{\partial x^2} + \mathrm{GI}\frac{k_d}{x}\frac{\partial T}{\partial x}. \tag{7}$$

Eq. (1) enables the evaluation of the freezing stage by means of the use of physical properties which are variable with temperature (the model uses apparent heat capacity that involves both sensible specific heat and the enthalpy of ice solidification), or the storage stage using the corresponding properties of frozen food.

In Eq. (7), the model uses the physical properties corresponding to the dehydrated food.

For the energy balance, besides Eq. (3), the following boundary conditions can be stated

$$x = x_1: \qquad -k\frac{\partial T}{\partial x} = L_s m_s \frac{dx_1}{dt} - k_d\frac{\partial T}{\partial x}, \tag{8}$$

$$x = L: \qquad -k_d\frac{\partial T}{\partial x} = h(T - T_a). \tag{9}$$

Ice sublimation takes place within the frozen zone, leading to a dried layer with a porous structure. Thus, there is a water vapour transfer to the surrounding medium through this layer. It should be stressed, that a fraction of the ice, f_{ads}, remains adsorbed to the food matrix, its value depending on the local vapour–ice equilibrium conditions (Chumak & Sibiriakov, 1988).

Vapour flow can be considered mainly as a diffusive flow passing throughout the dried layer, being the driving force in the difference in water vapour pressure between the sublimation front and the environment. Fick's law was considered valid.

The microscopic mass balance applied to this zone ($x_1 < x \leqslant L$) was as follows:

$$\varepsilon\frac{\partial C_{va}}{\partial t} = \frac{\partial D_{ef}}{\partial x}\frac{\partial C_{va}}{\partial x} + D_{ef}\frac{\partial^2 C_{va}}{\partial x^2} + \mathrm{GI}\frac{D_{ef}}{x}\frac{\partial C_{va}}{\partial x}. \tag{10}$$

Boundary conditions for the mass balance were, besides Eq. (5)

$$x = x_1: \qquad C_{va} = \frac{P_{sat}(T)}{R_g T}, \tag{11}$$

$$x = L: \qquad -D_{ef}\frac{\partial C_{va}}{\partial x} = k_m(C_{va} - C_a). \tag{12}$$

To evaluate the position of the sublimation front (and the thickness of the dehydrated layer) the model establishes that, at $x = x_1$

$$-m_s\frac{dx_1}{dt} = -D_{ef}\frac{\partial C_{va}}{\partial x} \quad \text{where } m_s = \rho(w - f_{ads}(1 - Y_0)). \tag{13}$$

3. Numerical model

Eqs. (1) and (2), or (1), (7), (10) and (13) lead to a system of coupled non-linear partial differential equations. The system is solved by an implicit finite-differences method (Crank–Nicolson centred method). In the dehydrated zone, a variable grid is applied to overcome the deformation of the original fixed grid due to the shift of the sublimation front. The finite differences generated are

$$\frac{\partial U}{\partial t} = \frac{U_i^{n+1} - U_i^n}{\Delta t}, \tag{14}$$

$$\frac{\partial U}{\partial x} = \frac{U_{i+1}^{n+1} - U_{i-1}^{n+1} + U_{i+1}^n - U_{i-1}^n}{4\Delta x}, \tag{15}$$

$$\frac{\partial^2 U}{\partial x^2} = \frac{U_{i+1}^{n+1} + U_{i-1}^{n+1} - 2U_i^{n+1} + U_{i+1}^n + U_{i-1}^n - 2U_i^n}{2\Delta x^2}, \tag{16}$$

where U is the temperature or concentration, i the node position and n is the time interval.

The domain has been discretized as it is shown in Fig. 1, where 0 indicates the food centre, m indicates the sublimation front (the point m moves with time) and b

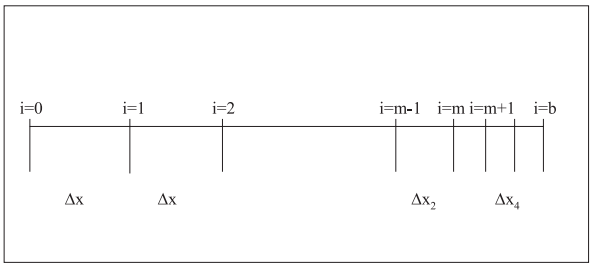

Fig. 1. Scheme of the discretization grid.

indicates the surface. The numerical model uses three different spatial increments:

- Δx: Constant spatial increment of the frozen–unfrozen area.
- Δx_2: Variable spatial increment (corresponds to the first increment within the frozen zone, and withdraws according to the advance of the sublimation front).
- Δx_4: Variable spatial increment, in the dehydrated area.

Assuming that thermal conductivity and the diffusion coefficient have a negligible change between times n and $(n+1)\ \Delta t$,

$$\frac{\partial V}{\partial x} = \frac{V_{i+1}^n - V_{i-1}^n}{2\Delta x}, \tag{17}$$

where V is the thermal conductivity or diffusion coefficient.

The complete set of algebraic equations obtained when replacing the finite-difference approximations into the original balances, including the adequate boundary conditions, is presented in Appendix A.

The whole equation system was solved, for each time step, following a pre-established order. Step 1 was solved firstly, temperature as well as concentration equations. When freezing begins, step 2 was solved. Temperature equations for both unfrozen–frozen and dehydrated zones were solved firstly. Then, the ice fraction was computed at the internal points. Afterwards, the vapour concentration profile within the dehydrated zone was computed. Then, the new front position and the new values of variables increments Δx_2 and Δx_4 were calculated to feedback these values into the system of temperature equations corresponding to the new time. After calculating the new position of the sublimation front, the model evaluates the dehydrated layer thickness and the weight loss. All the equation systems (for temperatures and concentrations, in steps 1 and 2) were tridiagonal, so they were solved using Thomas' Algorithm.

The weight loss as function of time is evaluated accumulating the instant loss calculated for each time step. Eq. (18) corresponds to step 1 and Eq. (19) to step 2.

$$\mathrm{WL1} = \frac{k'_{\mathrm{m}} A \Delta t \left(C_{\mathrm{wL}}^n - C_{\mathrm{eq}}\right)}{\rho_{\mathrm{i}} \mathrm{Vol}}, \tag{18}$$

$$\mathrm{WL2} = \frac{k_{\mathrm{m}} A \Delta t \left(C_{\mathrm{va\,L}}^n - C_{\mathrm{a}}\right)}{\rho_{\mathrm{i}} \mathrm{Vol}}. \tag{19}$$

4. Results

4.1. Theoretical predictions

The ability of the numerical software to predict temperature and concentration profiles inside the food and water loss as a function of time was used to analyse the influence of the operating conditions (air rate, humidity and temperature) and food characteristics on the freezing time and weight loss.

The conditions analysed were:

- *Air temperature*: Both freezing time and weight loss strongly depended on air temperature, the lower the temperature the faster the freezing and the lower the weight loss.
- *Air rate*: The air velocity affects both the heat transfer coefficient and the mass transfer coefficient. The effect is most important at low rate values, but freezing times and weight losses become independent of air rate for higher rate values.
- *Relative humidity*: One of the most important factors affecting the weight loss is the relative humidity, because it determines the driving force for evaporation and sublimation. Our results show a linear increase of weight loss as relative humidity.
- *Food thickness*: The effect of product thickness was analysed. Opposed effects were found, when thickness increased freezing time strongly increased, however, weight loss slightly decreased.

These theoretical results are presented in detail in Campañone, Salvadori, and Mascheroni (1998).

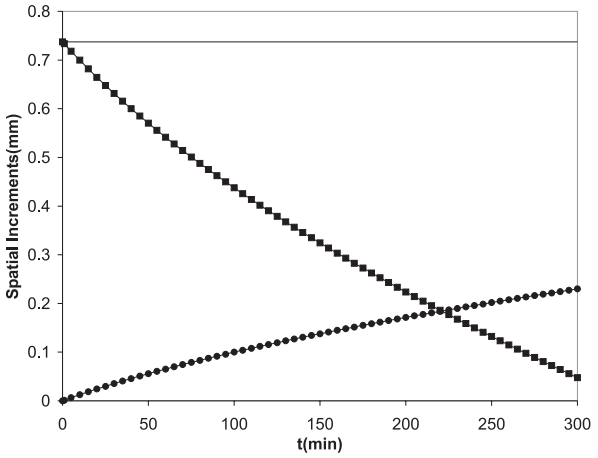

Fig. 2. Spatial increments Δx, Δx_2 and Δx_4. Their variation with time. — Δx, ■ Δx_2; ● Δx_4

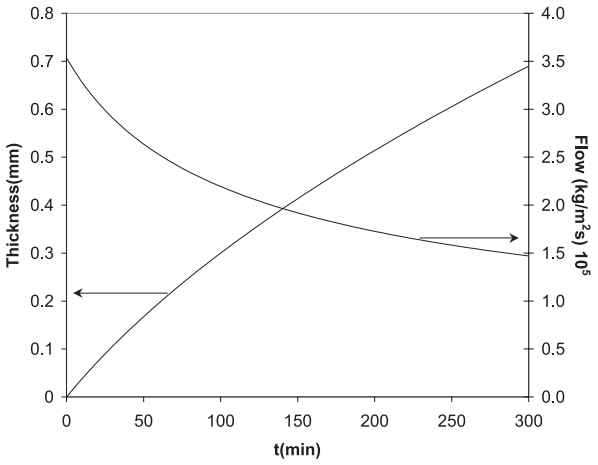

Fig. 3. Dehydrated layer thickness and sublimation flow vs time.

Moreover, one of the most significant contributions of this model is to estimate the depth of the dehydrated layer along the freezing and/or storage processes. On the contrary, other works on the subject assume a dehydrated layer of constant depth, this numerical model predicts the advance of the sublimation front alongside time. The predicted influence of process variables on the value of Δx_1 (the depth of the dehydrated layer) is completely equivalent to the results of weight loss (as they are directly related). To trace the movement of the sublimation front, the numerical method makes use of a variable grid. Even though the three space increments can vary with time, normally only Δx_2 and Δx_4 vary as is shown in Fig. 2, for meat samples and for conditions C1 (Table 2). Fig. 3 shows the development of the dehydrated layer for the same freezing conditions. In the same figure, the sublimation vapour flow as a function of time has been plotted. It is observed that this flow is variable in time, decreasing continuously as the depth of the dehydrated layer increases (for those methods that consider a constant dehydrated layer the predicted vapour flow is also constant).

4.2. Validation against experimental data

When the model predictions are intended to be verified against experimental data, it is found that there is no literature on weight loss during the freezing of individual products under controlled conditions. Only average values given by general textbooks or equipment leaflets can be found (Löndahl, Göransson, Sundstén, Andersson & Tornberg (1995)).

Two types of validations were performed.

4.2.1. Freezing stage

As there was no data about the simultaneous determination of freezing time and weight loss, only freezing time data of meat balls from Tocci and Mascheroni (1995b) were simulated. Table 1 shows the operating conditions for each run as well the experimental and numerical freezing time. The percentage error oscillates between 3.17% and −10.73%. The good agreement between experimental and numerical results demonstrated the accuracy of the developed prediction method. The

Table 1

Experimental conditions				Numerical method		
T_a (°C)	T_i (°C)	h (W/m^2 °C)	Freezing time, exp (min)	Freezing time, pred (min)	Error (%)	Weight loss (%)
−30.2	6.6	66.5	21.0	20.76	−1.14	1.08
−26.0	13.9	66.5	27.6	26.16	−5.20	1.47
−28.9	11.2	59.3	25.2	24.19	−3.99	1.32
−28.9	1.4	59.3	22.7	22.39	−1.36	0.96
−24.8	6.6	59.1	28.9	28.27	−2.17	1.26
−25.0	7.6	59.1	29.4	28.19	−4.11	1.29
−26.7	0.8	55.6	26.0	25.55	−1.72	1.02
−23.3	−0.3	55.6	29.5	30.44	3.17	0.96
−30.0	17.7	48.2	28.5	29.20	2.47	1.47
−30.2	5.9	48.2	27.8	26.27	−5.50	1.17
−28.9	1.8	42.9	30.1	28.88	−3.99	1.08
−30.8	13.1	42.9	31.0	29.55	−4.66	1.41
−24.8	1.2	42.5	37.0	34.93	−5.60	1.20
−24.9	10.3	42.5	38.6	37.83	−1.99	1.47
−29.3	10.9	37.6	33.0	33.74	2.25	1.41
−28.9	13.1	37.6	36.3	34.95	−3.72	1.47
−30.5	19.0	29.4	44.8	41.48	−7.41	1.53
−30.8	10.4	29.4	41.0	38.02	−7.26	1.41
−24.9	10.1	21.1	68.5	61.15	−10.73	1.59
−23.7	1.3	21.1	66.3	60.40	−8.89	1.26

Table 2
Storage conditions (air temperature, air speed, relative humidity) and symbols of experimental data

Condition	Meat $L = 0.01475$ m	Tylose $L = 0.0125$ m	Potato $L = 0.0125$ m	Symbol
C1	−9°C, 2.5 m/s, 47%	−9°C, 2.5 m/s, 53%	−9°C, 2.5 m/s, 44%	■
C2	−9°C, 1.5 m/s, 52%	−9°C, 1.5 m/s, 47%	−9°C, 1.5 m/s, 40%	●
C3	−9°C, 0.5 m/s, 45%	−9°C, 0.5 m/s, 40%	−9°C, 0.5 m/s, 35%	▲
C4	−20°C, 2.5 m/s, 45%	−20°C, 2.5 m/s, 51%	−20°C, 2.5m/s, 42%	□
C5	−20°C, 1.5 m/s, 48%	−20°C, 1.5 m/s, 37%	−20°C, 1.5 m/s, 38%	○
C6	−20°C, 0.5 m/s, 49%	−20°C, 0.5 m/s, 35%	−20°C, 0.5 m/s, 40%	Δ
C7	−30°C, 2.5 m/s, 45%	−30°C, 2.5 m/s, 50%	−30°C, 2.5 m/s, 48%	×
C8	−30°C, 1.5 m/s, 45%	−30°C, 1.5 m/s, 37%	−30°C, 1.5 m/s, 50%	◆
C9	−30°C, 0.5 m/s, 40%	−30°C, 0.5 m/s, 48%	−30°C, 0.5 m/s, 60%	◇

predicted weight losses fall in the range reported by freezing equipment manufacturers.

4.2.2. Weight loss during storage

For the storage case, for foods with simple shapes (sphere, cylinder, plate), there are only experiences with meat, potato and tylose cylinders (Sukhwal & Aguirre Puente, 1983; Lambrinos & Aguirre Puente, 1983), which were simulated with the numerical method.

The experiences were carried under the operating conditions detailed in Table 2.

The physical properties of the different foods used in the numerical simulation are described in Table 3. For each run, the heat transfer coefficient was estimated with the correlations presented by Welty (1974) and the mass transfer coefficient was estimated from Sakly and Lambrinos (1989).

Fig. 4 shows the weight loss (predicted and experimental) for meat samples (cylinders), under the different storage conditions detailed in Table 2. The experimental data are from Sukhwal and Aguirre Puente (1983).

In a similar way, Fig. 5 shows the weight loss (predicted and experimental) for tylose samples (cylinders).

Fig. 6 shows the weight loss (predicted and experimental) for potato samples (cylinders). The experimental data are from Lambrinos and Aguirre Puente (1983).

In order to analyse the influence of the storage conditions, the results of Fig. 7 show the effect of the air speed on the weight loss. The experimental data correspond to meat samples, from Sukhwal and Aguirre Puente (1983), under the storage conditions detailed in Table 2. The values of weight loss increase with the air circulation speed. This is due to the fact that higher Re causes an increase of the mass transfer coefficient.

Besides, the effect of air temperature on weight loss was analysed. Such results are shown in Fig. 8, the data correspond to tylose samples. These data confirm that the higher the air temperature, the higher the weight loss.

The experimental data used in the calculations were obtained under different room temperatures and air speeds, and for different materials. The good accuracy of these predicted results shows that the developed mathematical model enables the adequate prediction of the behaviour of frozen foods stored under conditions which lead to surface ice sublimation.

5. Conclusions

We have developed a numerical model that solves the coupled heat and mass balances during freezing and frozen storage of unwrapped foods. It allows to evaluate the temperature profiles, the freezing time, the thickness of the dehydrated layer and the weight loss during freezing and storage.

The model is suitable for different foods (with the adequate physical properties) and different geometries (slab, cylinder and sphere).

The numerical results give a very good prediction of the experimental values.

Acknowledgements

Authors Salvadori and Mascheroni are Scientific Researchers and author Campañone is a Fellow, all from the National Research Council (CONICET) of Argentina. This research was supported by grants from CONICET, ANPCyT and Universidad Nacional de La Plata from Argentina.

Appendix A

By replacing Eqs. (14)–(17) in the corresponding balance the finite-differences equations were obtained.

A.1. Evaluation of the temperature profile

Step 1. The equations for temperatures are detailed for the most general situation (step 2). For the beginning of the simulation, when T is higher than T_{if} for all the food, the system of equations is reduced to Eqs. (A.1), (A.2) and (A.9), using k instead of k_d and Δx instead of Δx_4 in the last equation.

Table 3
Properties of foods used in the numerical model

Property	Meat	Tylose	Potato
Initial water content	0.74[a]	0.77[b]	0.8[c]
Initial freezing temperature	−1.0[a]	−0.6[b]	−0.6[b]
Density (fresh)	1053[a]	1006[a]	1070[c]
Density (frozen)	$1053/0.982 + 0.113\,Y_0 + 0.257\,(1 - Y_0)T^{-1}$[a]	939.6[a]	990[d]
Density (dehydrated)	1000[e]	1000[e]	1400[f]
Thermal conductivity (fresh)	$0.0866 + 0.501\,Y_0 + 5.0521 \times 10^{-4}\,Y_0\,T$[a]	0.55[b]	0.53[b]
Thermal conductivity (frozen)	$0.378 + 1.376\,Y_0 + 0.93\,T^{-1}$[a]	1.65[b]	1.9[b]
Thermal conductivity (dehydrated)	0.065[g]	0.05594[h]	0.060[i]
Specific heat (fresh)	$1448\,(1 - Y_0) + 4187\,Y_0$[a]	3653.3[b]	3420.56[b]
Apparent specific heat (frozen)	$3874 - 2534\,Y_0 + 902893\,(1 - Y_0)T^{-2}$[a]	$2028.61 + 135424\,T^{-2}$[b]	$1969.7 + 144720\,T^{-2}$[b]
Specific heat (dehydrated)	796[j]	875.76[k]	1143.61[l]
Ice content	$1.1866\,Y_0 - 0.1866 + 2.7013\,(1 - Y_0)\,T^{-1}$[m]	$0.875\,Y_0\,(1 + 0.6\,T^{-1})$[k]	$0.9\,Y_0\,(1 + 0.6\,T^{-1})$[k]
Ice adsorbed fraction	0.25[n]	0.25[n]	0.25[n]
Porosity (dehydrated)	0.74[g]	0.77[h]	0.8[o]
Tortuosity (dehydrated)	1.5[p]	1.0	1.23[c]
Diffusion coefficient of vapour in air	$(5.684552510^{-9}\,(T + 273.16)^{1.5})/(0.78917 - 2.131434810^{-3}(T + 273.16))$[q]		
Saturation vapour pressure of water	$133.329\,\exp(23.986059 - 6139.9094/T)$[r]		

[a] Sanz, Dominguez and Mascheroni (1987).
[b] Cleland and Earle (1984).
[c] Lombardi and Zaritzky (1996).
[d] Mohsenin (1980).
[e] Berlin, Kliman, and Pallansh (1966).
[f] Krokida, Zogzas, and Maroulis. (1997).
[g] Harper (1962).
[h] Saravacos and Pilsworth (1965).
[i] Wang and Brennan (1992).
[j] Polley, Snyder, and Kotnour (1980).
[k] Miles, Van Beek, and Veerkamp (1983).
[l] Wang and Brennan (1993).
[m] Mascheroni and Calvelo (1978).
[n] Chumak and Sibiriakov (1988).
[o] Krokida, Karathanos, and Maroulis (1998).
[p] Gros, Dussap, and González Méndez (1984).
[q] Bird, Stewart, and Lightfoot (1976).
[r] Fennema and Berny (1974).

Step 2. General equation to estimate temperatures of unfrozen–frozen zones, valid for $0 < i < m - 2$.

$$\begin{aligned}
&T_{i+1}^{n+1}\left(-\frac{k_i^n}{2\Delta x^2} - \frac{k_{i+1}^n - k_{i-1}^n}{8\Delta x^2} - \frac{\mathrm{GI}k_i^n}{4(i-1)\Delta x^2}\right)\\
&\quad + T_i^{n+1}\left(\frac{\rho_i^n \mathrm{Cp}_i^n}{\Delta t} + \frac{k_i^n}{\Delta x^2}\right)\\
&\quad + T_{i-1}^{n+1}\left(\frac{-k_i^n}{2\Delta x^2} + \frac{k_{i+1}^n - k_{i-1}^n}{8\Delta x^2} + \frac{\mathrm{GI}k_i^n}{4(i-1)\Delta x^2}\right)\\
&\quad = T_{i+1}^{n}\left(\frac{k_i^n}{2\Delta x^2} + \frac{k_{i+1}^n - k_{i-1}^n}{8\Delta x^2} + \frac{\mathrm{GI}k_i^n}{4(i-1)\Delta x^2}\right)\\
&\quad + T_i^{n}\left(\frac{\rho_i^n \mathrm{Cp}_i^n}{\Delta t} - \frac{k_i^n}{\Delta x^2}\right)\\
&\quad + T_{i-1}^{n}\left(\frac{k_i^n}{2\Delta x^2} - \frac{k_{i+1}^n - k_{i-1}^n}{8\Delta x^2} - \frac{\mathrm{GI}k_i^n}{4(i-1)\Delta x^2}\right). \qquad (A.1)
\end{aligned}$$

For the centre point ($i = 0$), using the boundary condition (3), it was obtained

$$\begin{aligned}
&T_0^{n+1}\left(\frac{\rho_0^n \mathrm{Cp}_0^n}{\Delta t} + \frac{(\mathrm{GI}+1)k_0^n}{\Delta x^2}\right) + T_1^{n+1}\left(\frac{-(\mathrm{GI}+1)k_0^n}{\Delta x^2}\right)\\
&\quad = T_1^{n}\left(\frac{(\mathrm{GI}+1)k_0^n}{\Delta x^2}\right) + T_0^{n}\left(\frac{\rho_0^n \mathrm{Cp}_0^n}{\Delta t} - \frac{(\mathrm{GI}+1)k_0^n}{\Delta x^2}\right). \qquad (A.2)
\end{aligned}$$

In point ($m - 1$), a discontinuity was produced because space increments towards the frozen zone were fixed (Δx); however, towards the food surface, grid increment (Δx_2) was variable. In this case, the finite differences of Eqs. (15)–(17) were replaced by Eqs. (A.3)–(A.5). So, the equation corresponding to $i = m - 1$ is obtained (Eq. (A.6)).

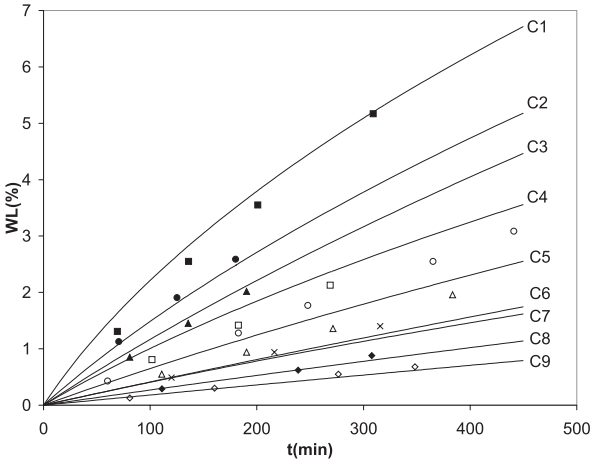

Fig. 4. Weight loss of meat samples. Full lines: calculated data (this work). Symbols: experimental data (Sukhwal & Aguirre Puente, 1983). Symbols: see Table 2.

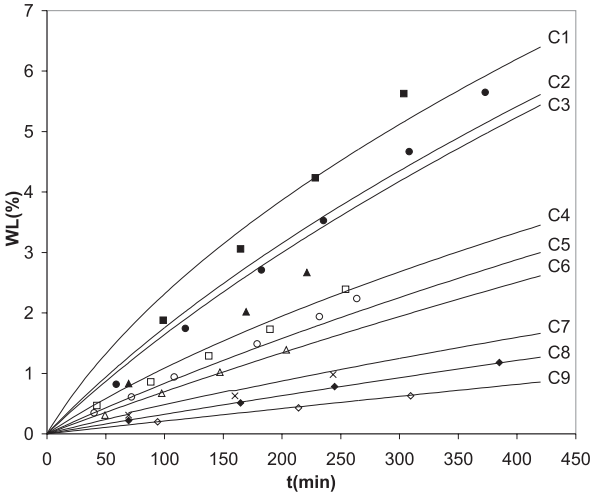

Fig. 5. Weight loss of tylose samples. Full lines: calculated data (this work). Symbols: experimental data (Sukhwal & Aguirre Puente, 1983). Symbols: see Table 2.

$$\frac{\partial T}{\partial x} = \frac{T_{i+1}^{n+1} - T_{i-1}^{n+1} + T_{i+1}^{n} - T_{i-1}^{n}}{2(\Delta x + \Delta x_2)}, \tag{A.3}$$

$$\frac{\partial^2 T}{\partial x^2} = \frac{2}{(\Delta x^2 + \Delta x_2^2)}\left(\frac{\left(T_{i+1}^{n+1} + T_{i+1}^{n}\right)\Delta x}{(\Delta x + \Delta x_2)} + \frac{\left(T_{i-1}^{n+1} + T_{i-1}^{n}\right)\Delta x_2}{(\Delta x + \Delta x_2)} - T_i^{n+1} - T_i^{n}\right), \tag{A.4}$$

$$\frac{\partial V}{\partial x} = \frac{V_{i+1}^{n} - V_{i-1}^{n}}{(\Delta x + \Delta x_2)}, \tag{A.5}$$

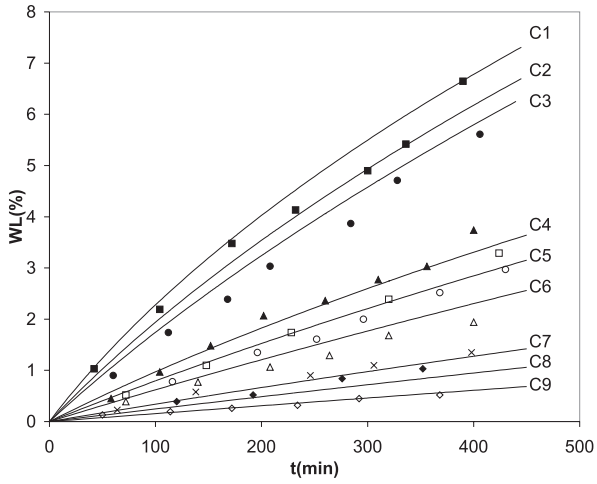

Fig. 6. Weight loss of potato samples. Full lines: calculated data (this work). Symbols: experimental data (Lambrinos & Aguirre Puente, 1983). Symbols: see Table 2.

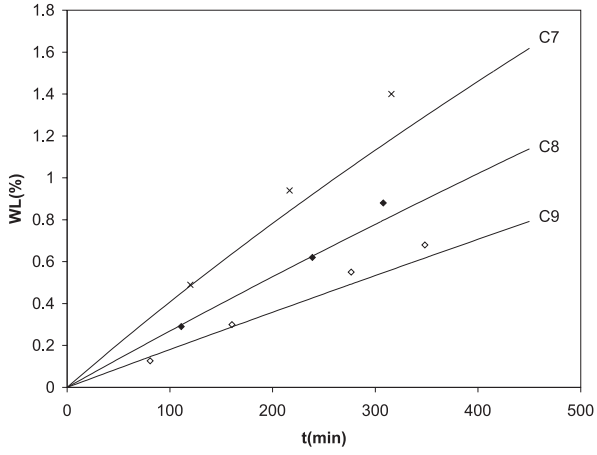

Fig. 7. Effect of the air speed on weight loss. Full lines: calculated data (this work). Symbols: experimental data (Sukhwal & Aguirre Puente, 1983). Symbols: see Table 2.

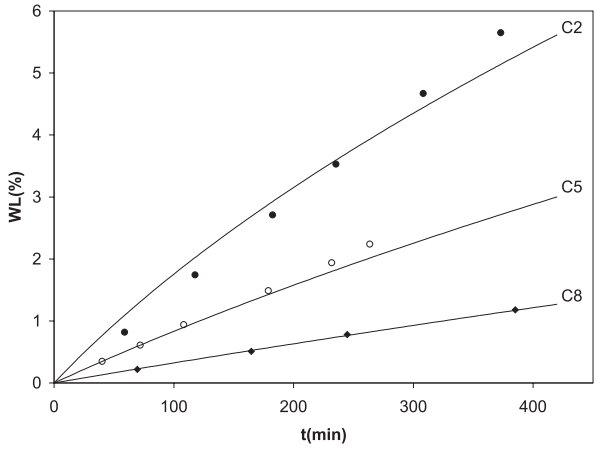

Fig. 8. Effect of air temperature on weight loss. Full lines: calculated data (this work). Symbols: experimental data (Sukhwal & Aguirre Puente, 1983). Symbols: see Table 2.

$$T_{i+1}^{n+1}\left(-\frac{2\Delta x k_i^n}{(\Delta x+\Delta x_2)(\Delta x^2+\Delta x_2^2)}-\frac{k_{i+1}^n-k_{i-1}^n}{2(\Delta x+\Delta x_2)^2}-\frac{\mathrm{GI}k_i^n}{2\Delta x(\Delta x+\Delta x_2)(i-1)}\right)+T_i^{n+1}\left(\frac{\rho_i^n \mathrm{Cp}_i^n}{\Delta t}+\frac{2k_i^n}{\Delta x^2+\Delta x_2^2}\right)+T_{i-1}^{n+1}\left(\frac{-2\Delta x_2 k_i^n}{(\Delta x+\Delta x_2)(\Delta x^2+\Delta x_2^2)}+\frac{k_{i+1}^n-k_{i-1}^n}{2(\Delta x+\Delta x_2)^2}+\frac{\mathrm{GI}k_i^n}{2\Delta x(\Delta x+\Delta x_2)(i-1)}\right)=T_{i+1}^n\left(\frac{2\Delta x k_i^n}{(\Delta x+\Delta x_2)(\Delta x^2+\Delta x_2^2)}+\frac{k_{i+1}^n-k_{i-1}^n}{2(\Delta x+\Delta x_2)^2}+\frac{\mathrm{GI}k_i^n}{2\Delta x(\Delta x+\Delta x_2)(i-1)}\right)+T_i^n\left(\frac{\rho_i^n \mathrm{Cp}_i^n}{\Delta t}-\frac{2k_i^n}{\Delta x^2+\Delta x_2^2}\right)+T_{i-1}^n\left(\frac{2\Delta x_2 k_i^n}{(\Delta x+\Delta x_2)(\Delta x^2+\Delta x_2^2)}-\frac{k_{i+1}^n-k_{i-1}^n}{2(\Delta x+\Delta x_2)^2}-\frac{\mathrm{GI}k_i^n}{2\Delta x(\Delta x+\Delta x_2)(i-1)}\right). \quad (A.6)$$

For the moving sublimation front ($i=m$), the condition (8) was used considering the two different spatial increments, Δx_2 and Δx_4. Eq. (A.7) is obtained for $i=m$

$$T_i^{n+1}\left(\frac{\rho_i^n \mathrm{Cp}_i^n}{\Delta t}+\frac{k_i^n}{2\Delta x_2^2}-\frac{k_{i+1}^n-k_{i-1}^n}{8\Delta x_2^2}-\frac{\mathrm{GI}k_i^n}{4\Delta x_2^2(i-1)}\right)+T_{i-1}^{n+1}\left(-\frac{k_i^n}{2\Delta x_2^2}+\frac{k_{i+1}^n-k_{i-1}^n}{8\Delta x_2^2}+\frac{\mathrm{GI}k_i^n}{4\Delta x_2^2(i-1)}\right)=T_i^n\left(\frac{\rho_i^n \mathrm{Cp}_i^n}{\Delta t}-\frac{k_i^n}{2\Delta x_2^2}+\frac{k_{i+1}^n-k_{i-1}^n}{8\Delta x_2^2}+\frac{\mathrm{GI}k_i^n}{4\Delta x_2^2(i-1)}\right)+T_{i-1}^n\left(\frac{k_i^n}{2\Delta x_2^2}-\frac{k_{i+1}^n-k_{i-1}^n}{8\Delta x_2^2}-\frac{\mathrm{GI}k_i^n}{4\Delta x_2^2(i-1)}\right)+\frac{k_{\mathrm{d}_i}^n(T_{i+1}^n-T_i^n)\Delta x_2}{k_i^n\Delta x_4}\left(\frac{k_i^n}{\Delta x_2^2}+\frac{k_{i+1}^n-k_{i-1}^n}{4\Delta x_2^2}+\frac{\mathrm{GI}k_i^n}{2\Delta x_2^2(i-1)}\right)+\frac{L_s m s_i^n \Delta x_1^n \Delta x_2}{\Delta t k_i^n}\left(-\frac{k_i^n}{\Delta x_2^2}-\frac{k_{i+1}^n-k_{i-1}^n}{4\Delta x_2^2}-\frac{\mathrm{GI}k_i^n}{2\Delta x_2^2(i-1)}\right). \quad (A.7)$$

To solve the energy balance in the dehydrated zone (Eq. (7)) the partial derivatives should be replaced by the finite differences (14)–(17). Thus, the general equation for the intermediate points ($m<i<b$) was obtained

$$T_{i+1}^{n+1}\left(-\frac{k_{\mathrm{d}_i}^n}{2\Delta x_4^2}-\frac{k_{\mathrm{d}_{i+1}}^n-k_{\mathrm{d}_{i-1}}^n}{8\Delta x_4^2}-\frac{\mathrm{GI}k_{\mathrm{d}_i}^n}{4(i-1)\Delta x_4^2}\right)+T_i^{n+1}\left(\frac{\rho_{\mathrm{d}_i}^n \mathrm{Cp}_{\mathrm{d}_i}^n}{\Delta t}+\frac{k_{\mathrm{d}_i}^n}{\Delta x_4^2}\right)+T_{i-1}^{n+1}\left(\frac{-k_{\mathrm{d}_i}^n}{2\Delta x_4^2}+\frac{k_{\mathrm{d}_{i+1}}^n-k_{\mathrm{d}_{i-1}}^n}{8\Delta x_4^2}+\frac{\mathrm{GI}k_{\mathrm{d}_i}^n}{4(i-1)\Delta x_4^2}\right)=T_{i+1}^n\left(\frac{k_{\mathrm{d}_i}^n}{2\Delta x_4^2}+\frac{k_{\mathrm{d}_{i+1}}^n-k_{\mathrm{d}_{i-1}}^n}{8\Delta x_4^2}+\frac{\mathrm{GI}k_{\mathrm{d}_i}^n}{4(i-1)\Delta x_4^2}\right)+T_i^n\left(\frac{\rho_{\mathrm{d}_i}^n \mathrm{Cp}_{\mathrm{d}_i}^n}{\Delta t}-\frac{k_{\mathrm{d}_i}^n}{\Delta x_4^2}\right)+T_{i-1}^n\left(\frac{k_{\mathrm{d}_i}^n}{2\Delta x_4^2}-\frac{k_{\mathrm{d}_{i+1}}^n-k_{\mathrm{d}_{i-1}}^n}{8\Delta x_4^2}-\frac{\mathrm{GI}k_{\mathrm{d}_i}^n}{4(i-1)\Delta x_4^2}\right). \quad (A.8)$$

For the food surface ($i=b$), the corresponding Eq. (A.9) was obtained by means of boundary condition (9)

$$T_i^{n+1}\left(\frac{\rho_{\mathrm{d}_i}^n \mathrm{Cp}_{\mathrm{d}_i}^n}{\Delta t}+\frac{k_{\mathrm{d}_i}^n}{\Delta x_4^2}+\frac{2h\Delta x_4}{k_{\mathrm{d}_i}^n}\left(\frac{k_{\mathrm{d}_i}^n}{2\Delta x_4^2}+\frac{k_{\mathrm{d}_{i+1}}^n-k_{\mathrm{d}_{i-1}}^n}{8\Delta x_4^2}+\frac{\mathrm{GI}k_{\mathrm{d}_i}^n}{4\Delta x_4^2(i-1)}\right)\right)+T_{i-1}^{n+1}\left(\frac{-k_{\mathrm{d}_i}^n}{\Delta x_4^2}\right)=T_i^n\left(\frac{\rho_{\mathrm{d}_i}^n \mathrm{Cp}_{\mathrm{d}_i}^n}{\Delta t}-\frac{k_{\mathrm{d}_i}^n}{\Delta x_4^2}+\frac{2h\Delta x_4}{k_{\mathrm{d}_i}^n}\left(-\frac{k_{\mathrm{d}_i}^n}{2\Delta x_4^2}-\frac{k_{\mathrm{d}_{i+1}}^n-k_{\mathrm{d}_{i-1}}^n}{8\Delta x_4^2}-\frac{\mathrm{GI}k_{\mathrm{d}_i}^n}{4\Delta x_4^2(i-1)}\right)\right)+T_{i-1}^n\left(\frac{k_{\mathrm{d}_i}^n}{\Delta x_4^2}\right)+\frac{2h\Delta x_4 T_a}{k_{\mathrm{d}_i}^n}\left(\frac{k_{\mathrm{d}_i}^n}{\Delta x_4^2}+\frac{k_{\mathrm{d}_{i+1}}^n-k_{\mathrm{d}_{i-1}}^n}{4\Delta x_4^2}+\frac{\mathrm{GI}k_{\mathrm{d}_i}^n}{2\Delta x_4^2(i-1)}\right). \quad (A.9)$$

A.2. Evaluation of the concentration profile

Step 1. General equation, for $0<i<b$

$$C_{\mathrm{w}_{i+1}}^{n+1}\left(\frac{-D_{\mathrm{w}_i}^n}{2\Delta x^2}-\frac{\left(D_{\mathrm{w}_{i+1}}^n-D_{\mathrm{w}_{i-1}}^n\right)}{8\Delta x^2}-\frac{\mathrm{GI}D_{\mathrm{w}_i}^n}{4\Delta x^2(i-1)}\right)+C_{\mathrm{w}_i}^{n+1}\left(\frac{1}{\Delta t}+\frac{D_{\mathrm{w}_i}^n}{\Delta x^2}\right)+C_{\mathrm{w}_{i-1}}^{n+1}\left(\frac{-D_{\mathrm{w}_i}^n}{2\Delta x^2}+\frac{\left(D_{\mathrm{w}_{i+1}}^n-D_{\mathrm{w}_{i-1}}^n\right)}{8\Delta x^2}+\frac{\mathrm{GI}D_{\mathrm{w}_i}^n}{4\Delta x^2(i-1)}\right)=C_{\mathrm{w}_{i+1}}^n\left(\frac{D_{\mathrm{w}_i}^n}{2\Delta x^2}+\frac{\left(D_{\mathrm{w}_{i+1}}^n-D_{\mathrm{w}_{i-1}}^n\right)}{8\Delta x^2}+\frac{\mathrm{GI}D_{\mathrm{w}_i}^n}{4\Delta x^2(i-1)}\right)+C_{\mathrm{w}_i}^n\left(\frac{1}{\Delta t}-\frac{D_{\mathrm{w}_i}^n}{\Delta x^2}\right)+C_{\mathrm{w}_{i-1}}^n\left(\frac{D_{\mathrm{w}_i}^n}{2\Delta x^2}-\frac{\left(D_{\mathrm{w}_{i+1}}^n-D_{\mathrm{w}_{i-1}}^n\right)}{8\Delta x^2}-\frac{\mathrm{GI}D_{\mathrm{w}_i}^n}{4\Delta x^2(i-1)}\right). \quad (A.10)$$

For the centre of the food, $i = 0$

$$C^{n+1}_{w_0}\left(\frac{1}{\Delta t}+\frac{(GI+1)D^n_{w_0}}{\Delta x^2}\right)+C^{n+1}_{w_1}\left(\frac{-(GI+1)D^n_{w_0}}{\Delta x^2}\right) = C^n_{w_1}\left(\frac{(GI+1)D^n_{w_0}}{\Delta x^2}\right)+C^n_{w_0}\left(\frac{1}{\Delta t}-\frac{(GI+1)D^n_{w_0}}{\Delta x^2}\right). \tag{A.11}$$

The point $i = b$ was evaluated using the boundary condition (12)

$$C^{n+1}_{w_i}\left(\frac{1}{\Delta t}+\frac{D^n_{w_i}}{\Delta x^2}+\frac{2k'_m\Delta x}{D^n_{w_i}}\left(\frac{D^n_{w_i}}{2\Delta x^2}+\frac{\left(D^n_{w_{i+1}}-D^n_{w_{i-1}}\right)}{8\Delta x^2}+\frac{GID^n_{w_i}}{4\Delta x^2(i-1)}\right)\right)+C^{n+1}_{w_{i-1}}\left(\frac{-D^n_{w_i}}{\Delta x^2}\right) = C^n_{w_i}\left(\frac{1}{\Delta t}-\frac{D^n_{w_i}}{\Delta x^2}-\frac{2k'_m\Delta x}{D^n_{w_i}}\left(\frac{D^n_{w_i}}{2\Delta x^2}+\frac{\left(D^n_{w_{i+1}}-D^n_{w_{i-1}}\right)}{8\Delta x^2}+\frac{GID^n_{w_i}}{4\Delta x^2(i-1)}\right)\right)+C^n_{w_{i-1}}\left(\frac{D^n_{w_i}}{\Delta x^2}\right)+\frac{4C_{eq}k'_m\Delta x}{D^n_{w_i}}\left(\frac{D^n_{w_i}}{2\Delta x^2}+\frac{\left(D^n_{w_{i+1}}-D^n_{w_{i-1}}\right)}{8\Delta x^2}+\frac{GID^n_{w_i}}{4\Delta x^2(i-1)}\right). \tag{A.12}$$

Step 2. For the sublimation front, the vapour pressure is the saturation pressure. So, according to the ideal gas law

$$C^{n+1}_{va_m}=\frac{P_{sat}(T^{n+1}_m)}{R_gT^{n+1}_m}. \tag{A.13}$$

The general equation for $m < i < b$ is

$$C^{n+1}_{va_{i+1}}\left(\frac{-D^n_{ef_i}}{2\varepsilon\Delta x^2_4}-\frac{\left(D^n_{ef_{i+1}}-D^n_{ef_{i-1}}\right)}{8\varepsilon\Delta x^2_4}-\frac{GID^n_{ef_i}}{4\varepsilon\Delta x^2_4(i-1)}\right)+C^{n+1}_{va_i}\left(\frac{1}{\Delta t}+\frac{D^n_{ef_i}}{\varepsilon\Delta x^2_4}\right)+C^{n+1}_{va_{i-1}}\left(\frac{-D^n_{ef_i}}{2\varepsilon\Delta x^2_4}+\frac{\left(D^n_{ef_{i+1}}-D^n_{ef_{i-1}}\right)}{8\varepsilon\Delta x^2_4}+\frac{GID^n_{ef_i}}{4\varepsilon\Delta x^2_4(i-1)}\right) = C^n_{va_{i+1}}\left(\frac{D^n_{ef_i}}{2\varepsilon\Delta x^2_4}+\frac{\left(D^n_{ef_{i+1}}-D^n_{ef_{i-1}}\right)}{8\varepsilon\Delta x^2_4}+\frac{GID^n_{ef_i}}{4\varepsilon\Delta x^2_4(i-1)}\right)+C^n_{va_i}\left(\frac{1}{\Delta t}-\frac{D^n_{ef_i}}{\varepsilon\Delta x^2_4}\right)+C^n_{va_{i-1}}\left(\frac{D^n_{ef_i}}{2\varepsilon\Delta x^2_4}-\frac{\left(D^n_{ef_{i+1}}-D^n_{ef_{i-1}}\right)}{8\varepsilon\Delta x^2_4}-\frac{GID^n_{ef_i}}{4\varepsilon\Delta x^2_4(i-1)}\right). \tag{A.14}$$

The point $i = b$ was evaluated using the boundary condition (12).

$$C^{n+1}_{va_i}\left(\frac{1}{\Delta t}+\frac{D^n_{ef_i}}{\varepsilon\Delta x^2_4}+\frac{2k_m\Delta x_4}{D^n_{ef_i}}\left(\frac{D^n_{ef_i}}{2\varepsilon\Delta x^2_4}+\frac{\left(D^n_{ef_{i+1}}-D^n_{ef_{i-1}}\right)}{8\varepsilon\Delta x^2_4}+\frac{GID^n_{ef_i}}{4\varepsilon\Delta x^2_4(i-1)}\right)\right)+C^{n+1}_{va_{i-1}}\left(\frac{-D^n_{ef_i}}{\varepsilon\Delta x^2_4}\right) = C^n_{va_i}\left(\frac{1}{\Delta t}-\frac{D^n_{ef_i}}{\varepsilon\Delta x^2_4}-\frac{2k_m\Delta x_4}{D^n_{ef_i}}\left(\frac{D^n_{ef_i}}{2\varepsilon\Delta x^2_4}+\frac{\left(D^n_{ef_{i+1}}-D^n_{ef_{i-1}}\right)}{8\varepsilon\Delta x^2_4}+\frac{GID^n_{ef_i}}{4\varepsilon\Delta x^2_4(i-1)}\right)\right)+C^n_{va_{i-1}}\left(\frac{D^n_{ef_i}}{\varepsilon\Delta x^2_4}\right)+\frac{4C_ak_m\Delta x_4}{D^n_{ef_i}}\left(\frac{D^n_{ef_i}}{2\varepsilon\Delta x^2_4}+\frac{\left(D^n_{ef_{i+1}}-D^n_{ef_{i-1}}\right)}{8\varepsilon\Delta x^2_4}+\frac{GID^n_{ef_i}}{4\varepsilon\Delta x^2_4(i-1)}\right). \tag{A.15}$$

The new position of the sublimation font was calculated by Eq. (13), transformed in Eq. (A.16) using the finite differences

$$-m^n_{s_i}\frac{(x^{n+1}_1-x^n_1)}{\Delta t}=-D^n_{ef_i}\left(\frac{C^{n+1}_{va_{m+1}}-C^{n+1}_{va_m}}{\Delta x_4}\right)\Rightarrow x^{n+1}_1 = x^n_1+\frac{D^n_{ef_i}(C^{n+1}_{va_{m+1}}-C^{n+1}_{va_m})\Delta t}{m^n_{s_i}\Delta x_4}. \tag{A.16}$$

References

Aguirre Puente, J., Frémond, M., & Comini, G. (1978). Freezing of soils-physical study and mathematical models. *International Journal of Refrigeration*, *1*, 99–106.

Aguirre Puente, J., & Sukhwal, R. N. (1983). Sublimation of ice in frozen dispersed media. In *Proceedings of the Third International Offshore Mechanics and Arctic Engineering Symposium* (pp. 38–44), vol. 3.

Berlin, E., Kliman, P. G., & Pallansh, M. J. (1966). Surface areas and densities of freeze dried foods. *Journal of Agricultural Food Chemistry*, *14*, 15–17.

Bird, R. B., Stewart, W. E., & Lightfoot, E. N. (1976). *Transport phenomena*. New York: Wiley.

Campañone, L. A., Salvadori, V. O., & Mascheroni, R. H. (1998). Finite differences method to solve the coupled heat and mass balances during freezing with simultaneous surface dehydration. In S. Idelsohn, E. Oñate, E. Dvorkin, *Computational Mechanics: New Trends and Applications* (pp. 1–19), CIMNE, Barcelona, Compact Disc, I, vol. 1–8.

Cleland, A. C. (1990). *Food refrigeration processes. Analysis, design and simulation*. London: Elsevier.

Cleland, A. C., & Earle, R. L. (1984). Assessment of freezing time prediction methods. *Journal of Food Science*, *49*, 1034–1042.

Chumak, I. G., & Sibiriakov, P. V. (1988). Influence of air parameters in a frigorific chamber on the humidity content of the surface of meat during refrigeration. *Izvestia vuzov Pischevaia tejnologuia*, *2*, 54–56 (Russian).

Fennema, O., & Berny, L. A. (1974). Equilibrium vapour pressure and water activity of food at subfreezing temperature. In *Proceedings of IV International Congress of Food Science and Technology* (pp. 27–35), vol. 2.

Gros, J. B., Dussap, C. G., & González–Méndez, N. (1984). Solute diffusivities in meat – a review. In B. McKenna, *Engineering and Food* (pp. 287–297), vol. 1. London: Elsevier.

Harper, J. (1962). Transport properties of gases in porous media at reduced pressures with reference to freeze-drying. *AIChE Journal*, *8*, 298–302.

Kochs, M., Körber, Ch., Nunner, B., & Heschel, I. (1991). The influence of the freezing process on vapour transport during sublimation in vacuum-freeze-drying. *International Journal of Heat and Mass Transfer*, *34*, 2395–2408.

Krokida, M. K., Karathanos, V. T., & Maroulis, Z. B. (1998). Effect of freeze-drying conditions on shrinkage and porosity of dehydrated agricultural products. *Journal of Food Engineering*, *35*, 369–380.

Krokida, M. K., Zogzas, N. P., & Maroulis, Z. B. (1997). Modelling shrinkage and porosity during vacuum dehydration. *International Journal of Food Science and Technology*, *32*, 445–458.

Lambrinos, G. P., & Aguirre Puente, J. (1983). Deshydratation des milieux dispersés congelés. Influence des conditions d'entreposage sur les pertes de masse. In *Proceedings of the XVI International Congress of Refrigeration* (pp. 567–573), vol. 2.

Lombardi, A. M., & Zaritzky, N. E. (1996). Simultaneous diffusion of citric acid and ascorbic acid in prepeeled potatoes. *Journal of Food Process Engineering*, *19*, 27–48.

Löndahl, G., Göransson, S., Sundstén, S., Andersson, A., & Tornberg, E. (1995). Quality differences in fast freezing. In *19th International Congress of Refrigeration* (pp. 197–204), vol. I.

Marshall, G., Rey, C., & Smith, L. (1986). Métodos de Seguimiento de la Interfase para problemas unidimensionales de frontera móvil II. *Revista Internacional de Métodos Numéricos para Cálculo y Diseño en Ingeniería*, *2*, 351–366.

Mascheroni, R. H., & Calvelo, A. (1978). Modelo de descenso crioscópico en tejidos cárneos. *La Alimentación Latinoamericana*, *12*, 34–42.

Méndez Bustabad, O. (1999). Weight loss during freezing and the storage of frozen meat. *Journal of Food Engineering*, *41*, 1–11.

Miles, C. A., van Beek, G., & Veerkamp, C. H. (1983). Calculation of thermophysical properties of foods. In *Physical Properties of Foods*. Barking: Applied Science Publishers (Chapter 16).

Mohsenin, N. (1980). *Thermal properties of foods and agricultural materials*. London: Gordon and Breach.

Pham, Q. T., & Willix, J. (1984). A model for food desiccation in frozen storage. *Journal of Food Science*, *49*, 1275–1281.

Polley, S. L., Snyder, O. P., & Kotnour, P. (1980). A compilation for thermal properties of foods. *Food Technology*, *34*, 76–94.

Sakly, M., & Lambrinos, G. (1989). Sublimation de la glace sous convection forcée. Determination du coefficient global de transfert de masse. *International Communications Heat and Mass Transfer*, *16*, 633–644.

Sanz, P. D., Dominguez, M., & Mascheroni, R. H. (1987). Thermophysical properties of meat products. General bibliography and experimental data. *Transactions of the ASAE*, *30*, 283–296.

Saravacos, G. D, & Pilsworth, J. R. (1965). Thermal conductivities of freeze-dried model food gels. *Journal of Food Science*, *30*, 773–778.

Sukhwal, R. N., & Aguirre Puente, J. (1983). Sublimation des milieux dispersés. Considerations theoriques et experimentation. *Revue General Thermique*, *262*, 663–673.

Tocci, A. M., & Mascheroni, R. H. (1995a). Numerical models of the simultaneous heat and mass transfer during food freezing and storage. *International Communications in Heat and Mass Transfer*, *22*, 251–260.

Tocci, A. M., & Mascheroni, R. H. (1995b). Freezing times of meat balls in belt freezers: experimental determination and prediction by different methods. *International Journal of Refrigeration*, *17*, 445–452.

Wang, N., & Brennan, J. G. (1992). Thermal conductivity of potato as a function of moisture content. *Journal of Food Engineering*, *17*, 153–160.

Wang, N., & Brennan, J. G. (1993). The influence of moisture content and temperature on the specific heat of potato measured by differential scanning calorimetry. *Journal of Food Engineering*, *19*, 303–310.

Welty, J. R. (1974). *Engineering Heat Transfer* (pp. 254–275). New York: Wiley.